Trinucleon magnetic moments

E. L. Tomusiak and M. Kimura
Saskatchewan Accelerator Laboratory and Department of Physics, University of Saskatchewan, Saskatoon, Saskatchewan, Canada S7N 0W0

J. L. Friar and B. F. Gibson
Theoretical Division, Los Alamos National Laboratory, Los Alamos, New Mexico 87545

G. L. Payne
Department of Physics and Astronomy, University of Iowa, Iowa City, Iowa 52242

J. Dubach
Department of Physics and Astronomy, University of Massachusetts, Amherst, Massachusetts 01003
(Received 8 July 1985)

Impulse approximation and pion-exchange current contributions to the trinucleon magnetic moments are calculated using wave functions generated by solving the configuration-space Faddeev equations for a variety of nucleon-nucleon force models. Careful attention is paid to the origin of important exchange current contributions. Numerical results are compared with previously published calculations and with the experimental data. An attempt is made to isolate and understand sources of discrepancy between our results and those previously published. Calculations which include both impulse and pion-exchange current contributions are in fairly good agreement with experiment, whereas calculations which include only the impulse approximation term are not.

I. INTRODUCTION

The study of nuclear magnetic moments has played an important role in our understanding of nuclear forces. Deviations from the Schmidt limits gave an early indication of deficiencies in the extreme single-particle model. Apart from the suggestion that nuclear collective motion was the cause, another possibility lay in the quenching of nucleon moments inside nuclear matter.[1] The intriguing aspect of quenching is that it offers a window into the modification of nuclear properties due to subnuclear degrees of freedom. In today's parlance, subnuclear degrees of freedom are referred to as meson exchange currents (MEC's) or, more recently, as quark percolation or deconfinement effects, although calculations of the latter are only qualitative. Unfortunately, for most of the periodic table the uncertainties which arise in theoretical treatments of the many-body problem make it difficult to ascribe differences between calculated and measured magnetic moments as due to subnuclear effects.

The few-nucleon systems ^{2}H, ^{3}He, and ^{3}H are free of nuclear structure uncertainties associated with the difficulty of solving a multinucleon Schrödinger equation. That is, given a nucleon-nucleon (NN) potential, the wave functions for these nuclei can, in principle, be computed to arbitrary numerical precision. Therefore these nuclei have played an all-important role in elucidating the character of meson exchange currents. In the case of the deuteron, explanation of the magnetic moment does not appear to require exchange currents at the few percent level. This says only that *isoscalar* MEC's are small, a fact in agreement with current understanding[2] which says that isoscalar MEC's are of the same order as relativistic corrections. It was in the process of radiative n-p capture where the real importance and size of isovector MEC's was immediately apparent. The 1972 paper by Riska and Brown[3] demonstrated that including isovector MEC's could remove the 10% discrepancy (in the capture rate) between experiment and impulse approximation theory. Apart from some refinements, these same MEC's play an important role in accounting for the inelastic M1 form factors measured in the ^{2}H(e,e')np reaction.[4]

A measurement of the magnetic moments of ^{3}He and ^{3}H was encouraged by Sachs and Schwinger[5] in 1946. At that time, the interest in such a measurement was to determine the deviations from L-S coupling in these nuclei. For example, Gerjuoy and Schwinger[6] had predicted an admixture of four percent $^4D_{1/2}$ state to the predominantly pure $^2S_{1/2}$ ground state. Using this wave function, Sachs and Schwinger predicted trinucleon magnetic moments which were closer to the (then unknown) experimental values than are given by similar (impulse approximation) calculations today. Modern trinucleon wave functions reflect the increased sophistication both in NN potentials and in computing power compared to that available in the 1940's. However, as will be seen in what follows, contemporary impulse approximation calculations of the trinucleon magnetic moments give results nearly 20% different from the measured values. Most of this difference is expected to be explained by MEC's.

Calculations of MEC corrections to trinucleon magnetic moments and form factors using modern potentials and Faddeev wave functions can be traced back to the early 1970's. One of the first papers was the work by Harper,

Kim, Tubis, and Rho[7] in 1972. Phenomenological wave functions were used by Riska,[8] while Maize and Kim,[9] Strueve *et al.*,[10] and Torre and Goulard[11] used wave functions generated by Faddeev methods. All agreed on the dominant processes contributing to the MEC corrections—processes in which a pion is exchanged between two nucleons. They differed somewhat in their treatment of the contributions of heavier meson (i.e., ρ and ω) exchange. Strueve *et al.*, for example, included a more complete treatment of terms which involve virtual excitation of the $\Delta(3,3)$ isobar. When compared to the dominant pion exchange terms, heavy-meson effects contribute at the order of 10%, and their reliable calculation is problematical. Much of this suppression results because the trinucleon wave functions become very small at nucleon-nucleon separations corresponding to the range of the heavy mesons.

Although previous groups agreed on the dominant MEC diagrams (see Fig. 1) contributing to the trinucleon magnetic moments (basically the same diagrams considered by Riska and Brown), they did not always agree on the numerical values. We believe it is important to establish these values as well as possible. There is little point in computing higher-order corrections, or heavy-meson exchange terms, unless one has confidence in the size of the major effects. In this paper, we present a careful, detailed analysis of these MEC corrections to the trinucleon magnetic moments. Whenever possible, we will emphasize agreement with previous work or attempt to explain any lack thereof. Our calculations are performed using six different NN potential models. In this way the dependence of the magnetic moments on binding effects, for example, can be partially explored.

The presentation is as follows. In Sec. II we give general formulae for the magnetic moments in terms of the nuclear current density. Also presented here are our impulse approximation results for the six NN potentials considered in this paper. These potential models are the Reid soft core (RSC),[12] the Argonne V_{14} (AV14),[13] the super soft core C (SSCC),[14] the de Tourreil-Rouben-Sprung B (TRS),[15] the Malfliet-Tjon I–III (MT13),[16] and the RSC with Coulomb potential (RSCC).[17] Ground-state trinucleon properties resulting from these potentials are given in Refs. 17, 18, and 19. In Secs. III, IV, and V, we deal separately with each of the main MEC diagrams—the pair diagram, the pion diagram, and the Δ-isobar diagram. In each section, we compare our results with those of earlier publications. Finally, in Sec. VI, we conclude with a summary of calculated trinucleon magnetic moments.

II. GENERAL FORMULAE AND IMPULSE APPROXIMATION

The current density at the point $\mathbf{r}$ is denoted by $\mathbf{J}(\mathbf{r})$. We define a magnetic dipole density $\rho_{\rm mag}(r)$ by means of

$$\rho_{\rm mag}(r)=\tfrac{1}{2}\int d\Omega[\mathbf{r}\times\mathbf{J}(\mathbf{r})]_z \ , \tag{1}$$

so that the magnetic dipole form factor $\mu(q)$ is given by

$$\mu(q)=\int_0^\infty \left[\frac{3j_1(qr)}{(qr)}\right]\rho_{\rm mag}(r)r^2dr \ . \tag{2}$$

The static magnetic moments are then given by

$$\mu=\int_0^\infty \rho_{\rm mag}(r)r^2dr \ . \tag{3}$$

Thus, the magnetic moment is just the volume integral (apart from a factor of 4π) of the magnetic dipole density. Each process contributing to $\mathbf{J}(\mathbf{r})$ will generate its own contribution to $\rho_{\rm mag}(r)$.

In the impulse approximation, the current density arises from convection currents $\mathbf{J}_c$ and magnetization currents $\mathbf{J}_{\rm mag}$ where

$$\mathbf{J}_c(\mathbf{r})=\frac{1}{2M_{\rm p}}\sum_i\left[\frac{1+\tau_3(i)}{2}\right][\mathbf{p}_i\delta(\mathbf{r}-\mathbf{x}_i)+\delta(\mathbf{r}-\mathbf{x}_i)\mathbf{p}_i] \tag{4}$$

and

$$\mathbf{J}_{\rm mag}(\mathbf{r})=\nabla\times\sum_i\left[\frac{1+\tau_3(i)}{2}\mu_{\rm p}+\frac{1-\tau_3(i)}{2}\mu_{\rm n}\right]\times\boldsymbol{\sigma}(i)\delta(\mathbf{r}-\mathbf{x}_i) \ . \tag{5}$$

In Eq. (5), $\mu_{\rm p}$ ($=2.793\ \mu_{\rm N}$) and $\mu_{\rm n}$ ($=-1.913\ \mu_{\rm N}$) are the free proton and neutron magnetic moments in nuclear magnetons ($e\hbar/2M_{\rm p}c$).

The contribution of $\mathbf{J}_{\rm mag}$ to $\rho_{\rm mag}$ splits naturally into two pieces: $\rho_\sigma(r)$, directly proportional to the magnetic spin density $\sum_i\mu(i)\sigma_z(i)$, and $\rho_{Y\sigma}$, proportional to the product operator $\sum_i\mu(i)[Y_2(\hat{r})\otimes\sigma(i)]^1_0$. From $\mathbf{j}_c$ arises a term ρ_{L_z} proportional to the operator $\sum_i e(i)L_z(i)$. The impulse approximation to $\rho_{\rm mag}$ takes the form

$$\rho^{\rm imp}_{\rm mag}=\rho_{L_z}+\rho_{Y\sigma}-\tfrac{1}{3}r\frac{d}{dr}(\rho_\sigma-\rho_{Y\sigma}) \ , \tag{6}$$

and the corresponding magnetic moment becomes (after an integration by parts)

$$\mu^{\rm imp}=\int_0^\infty r^2(\rho_\sigma+\rho_{L_z})dr \ . \tag{7}$$

We note that $\rho_{Y\sigma}$ does not contribute to μ although we shall see later that it makes a non-negligible contribution to $\rho_{\rm mag}(r)$. The reader should note that we have assumed point nucleons. The charges $e(i)$ and the nucleon magnetic moments $\mu(i)$ must be replaced by the appropriate nucleon form factors when computing $\mu(q\neq0)$.

It is useful to examine how the densities ρ_σ, ρ_{L_z}, and $\rho_{Y\sigma}$ depend on the various wave function components. All our calculations have been performed using a five-channel Faddeev approximation: only the dominant two-nucleon partial waves $^1S_0$ and $^3S_1$-$^3D_1$ are retained. The corresponding L-S components in our trinucleon wave functions are $^2S_{1/2}$, $^2S'_{1/2}$, $^2P_{1/2}$, $^2P'_{1/2}$, $^4P_{1/2}$, and three $^4D_{1/2}$ components. For the notation, we refer the reader to the paper by Friar *et al.*[20] The formulae are cumbersome to write out in detail, especially if all the above components are included. We have, therefore, elected to suppress the small P wave parts from our formulae. Their effect has been included, however, in all numerical results. The formulae are

$$\rho_\sigma(r)=4\pi\int d^3x\,d^3y\,\delta(\mathbf{r}+\tfrac{2}{3}\mathbf{y})\left\{\frac{\mu_p+\mu_n}{2}[F_\sigma(u,v_1,v_2,v_3,v_4)-4uv_1]-(2T_3)\frac{\mu_p-\mu_n}{2}F_\sigma\left[u,v_1,i\frac{\sqrt{5}}{\sqrt{3}}v_2,iv_3,\frac{1}{\sqrt{3}}v_4\right]\right\}, \tag{8}$$

where

$$F_\sigma(u,v_1,v_2,v_3,v_4)=\{(u^2+v_1^2+v_2^2)-(1+3\mu^2)[(v_4^L)^2+(v_3^L)^2]$$
$$-3(1-\mu^2)[(v_4^M)^2+(v_3^M)^2]-(3+\mu^2)[(v_4^K)^2+(v_3^K)^2]-8\mu(v_4^Kv_4^L+v_3^Kv_3^L)\}\ .$$

All "radial functions" (i.e., u, v_1, etc.) depend on the three scalar quantities x, y, and $\mu=\hat{x}\cdot\hat{y}$. Here $\mathbf{x},\mathbf{y}$ are the usual Jacobi coordinates $\mathbf{x}=\mathbf{r}_2-\mathbf{r}_3$ and $\mathbf{y}=\frac{1}{2}(\mathbf{r}_2+\mathbf{r}_3)-\mathbf{r}_1$. The radial function u is associated with the spatially symmetric principal S state, v_1 and v_2 are associated with the mixed symmetry S state, while v_3 and v_4 are associated with the various families (L,M,N) of mixed symmetry D states. The quantity $(2T_3)$ has the values $+1$ and -1 for ^{3}He and ^{3}H, respectively. Corresponding expressions for ρ_{L_z} and $\rho_{Y\sigma}$ are given below:

$$\rho_{L_z}(r)=4\pi\int d^3x\,d^3y\,\delta(\mathbf{r}+\tfrac{2}{3}\mathbf{y})\left[\frac{e_p+e_n}{2}F_L(v_3,v_4)+(2T_3)\frac{e_p-e_n}{2}F_L\left[v_3,\frac{i}{\sqrt{3}}v_4\right]\right], \tag{9}$$

where

$$F_L(v_3,v_4)=\{(1+3\mu^2)[(v_3^L)^2+(v_4^L)^2]+3(1-\mu^2)[(v_3^M)^2+(v_4^M)^2]+(3+\mu^2)[(v_3^K)^2+(v_4^K)^2]$$
$$+8\mu(v_3^Kv_3^L+v_4^Kv_4^L)+2\mu(1-\mu^2)(v_4^L\overleftrightarrow{\partial}_\mu v_4^M+v_3^L\overleftrightarrow{\partial}_\mu v_3^M)-4(v_4^Lv_4^M+v_3^Lv_3^M)$$
$$+2(1-\mu^2)(v_4^K\overleftrightarrow{\partial}_\mu v_4^M+v_3^K\overleftrightarrow{\partial}_\mu v_3^M)-4\mu(v_4^Kv_4^M+v_3^Kv_3^M)\}$$

and where e_p and e_n $(=0)$ are the proton and neutron electric charges. We use the abbreviation

$$A\overleftrightarrow{\partial}_\mu B=A\frac{\partial B}{\partial\mu}-\frac{\partial A}{\partial\mu}B\ .$$

We also have

$$\rho_{Y\sigma}(r)=4\pi\int d^3x\,d^3y\,\delta(\mathbf{r}+\tfrac{2}{3}\mathbf{y})\left[\frac{\mu_p+\mu_n}{2}F_Y(u,v_1,v_2,v_3,v_4)+(2T_3)\frac{\mu_p-\mu_n}{2}F_Y\left[u,v_1,\frac{i}{\sqrt{3}}v_2,v_3,\frac{i}{\sqrt{3}}v_4\right]\right], \tag{10}$$

where

$$F_Y(u,v_1,v_2,v_3,v_4)=(1+3\mu^2)(uv_3^L-v_2v_4^L+v_1v_3^L)-3(1-\mu^2)(uv_3^M-v_2v_4^M+v_1v_3^M)$$
$$+4\mu(uv_3^K-v_2v_4^K+v_1v_3^K)+\tfrac{1}{2}(9\mu^2-1)[(v_3^L)^2+(v_4^L)^2]$$
$$-3(1-\mu^2)(v_4^Lv_4^M+v_3^Lv_3^M)+\mu(3\mu^2+5)(v_4^Lv_4^K+v_3^Lv_3^K)$$
$$+\tfrac{3}{2}(1-\mu^2)[(v_3^M)^2+(v_4^M)^2]-3\mu(1-\mu^2)(v_4^Mv_4^K+v_3^Mv_3^K)+\tfrac{1}{2}(3+5\mu^2)[(v_3^K)^2+(v_4^K)^2]\ . \tag{11}$$

Integration of the densities ρ_σ and ρ_{L_z} according to Eq. (7) does *not* yield an expression for μ in terms of configuration probabilities. The difficulty lies with terms in ρ_{L_z} which cannot be reduced to probabilities. We note, however, that if only one of the D-wave components is kept (i.e., K, L, or M), then the magnetic moment is given by

$$\mu=\frac{\mu_p+\mu_n}{2}[P(S)+P(S')-P(D)]$$
$$-(2T_3)\frac{\mu_p-\mu_n}{2}[P(S)-\tfrac{1}{3}P(S')+\tfrac{1}{3}P(D)]$$
$$+\tfrac{1}{2}P(D)[1+\tfrac{1}{3}(2T_3)]\ . \tag{12}$$

Here $P(S)$ is the probability of the principal S state, etc. Apart from the appearance of the probability of the mixed symmetry S state, $P(S')$, Eq. (12) is identical to that derived by Sachs and Schwinger in Ref. 5. However, as clearly pointed out by those authors, Eq. (12) holds only if P waves are neglected and only if just one form of the D wave is retained. (This formula has appeared in the literature as *the* impulse approximation result.) The error is not large, though, because the offending terms are in the L_z piece. For example, with the Reid soft core (RSC) potential model, Eq. (12) gives $\mu_s=0.404$ and $\mu_v=-2.139$ for the isoscalar and isovector magnetic moments. Numerical integration of Eq. (7), however, yields $\mu_s=0.404$ and $\mu_v=-2.149$. All of the results which we quote below were computed by numerical integration of ρ_{mag}.

We illustrate, using the RSC model, the impulse approximation isoscalar and isovector densities in Fig. 2. In this figure, we include in succession ρ_σ, ρ_{L_z}, and $\rho_{Y\sigma}$. The effect of ρ_{L_z} is almost too small to be noticeable, whereas

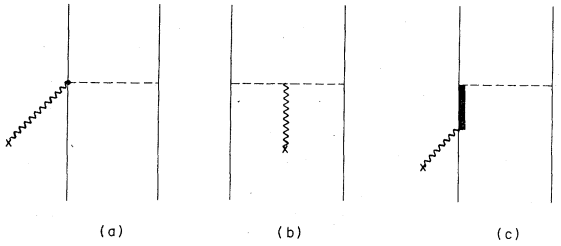

FIG. 1. (a) Seagull or pair diagram; (b) pion (true exchange) current diagram; (c) Δ-isobar diagram.

the addition of $\rho_{Y\sigma}$ to ρ_σ produces a marked change in the density. This is due to the S-D overlap which is allowed by the $[Y_2\otimes\sigma]^1$ operator. Of course, the addition of $\rho_{Y\sigma}$ still produces no change in μ but it does produce a significant change in the form factors. This is illustrated in Fig. 3. (Nucleon form factors are used in computing the curves of Fig. 3; however, for our purposes, it is not necessary to elaborate on these details.)

Table I lists our values of the trinucleon magnetic moments computed in the impulse approximation. Also tabulated are the results of Maize and Kim[9] (MK), Strueve, Hajduk, and Sauer[10] (SHS), Torre and Goulard[11] (TG), Torre, Goulard, and Hadjimichael[21] (TGH), and of Harper, Kim, Tubis, and Rho[7] (HKTR), all of which used RSC wave functions. In addition, we include the results of Hadjimichael, Goulard, and Bornais[22] (HGB) who used the TRS potential.

Several points should be made with respect to the entries in Table I. The magnetic moments computed with the MT13 potential are at variance with the others. This potential has no tensor force and hence there is no D wave in the ground state wave functions. We include it only for pedagogical purposes. The values of μ_s and μ_v computed by MK differ somewhat from ours. However, this may be a result of their using a parametrized wave function obtained by an approximate fit to the RSC wave function of Brandenburg *et al.*[23] The values of HKTR are in excellent agreement with our own. Finally, we note the values

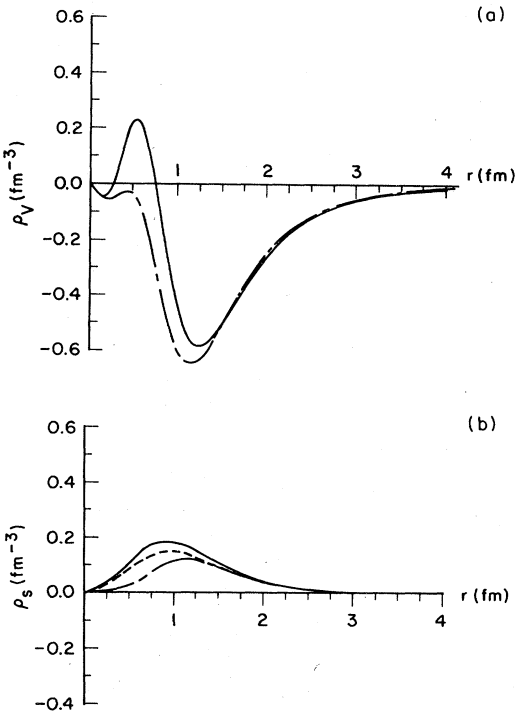

FIG. 2. (a) Impulse approximation isovector magnetic density. Dash-dot, dashed, and solid lines depict the densities computed using Eq. (6) and ρ_σ only, $\rho_\sigma+\rho_{L_z}$, and $\rho_\sigma+\rho_{L_z}+\rho_{Y\sigma}$, respectively. In this figure, the dash-dot and dashed curves are indistinguishable. (b) Impulse approximation isoscalar magnetic density. Labeling of curves as described for Fig. 1(a).

of TG appear to be at variance with the others. This is puzzling in view of the fact that there is agreement among HGB, TGH, and ourselves.

III. THE PAIR TERM

Derivations of the various exchange currents can be found in any one of several references.[24,25] The pair (or seagull) current [see Fig. 1(a)] is given by,

TABLE I. Impulse approximation magnetic moments.

Reference	Potential	μ_s	μ_v	$\mu(^3\text{He})$	$\mu(^3\text{H})$	Comments
	RSCC	0.405	−2.143	−1.738	2.547	Coulomb corrected
	RSC	0.405	−2.149	−1.744	2.553	
Present	AV14	0.405	−2.165	−1.760	2.571	
work	SSCC	0.409	−2.179	−1.769	2.588	
	TRS	0.407	−2.166	−1.759	2.573	
	MT13	0.440	−2.292	−1.852	2.732	S state only
MK	RSC	0.37	−2.19	−1.83	2.56	fit to RSC
SHS	RSC	0.40	−2.16	−1.76	2.56	18-channel
TG	RSC	0.397	−2.109	−1.711	2.506	
TGH	RSC	0.395	−2.127	−1.732	2.521	
HKTR	RSC	0.408	−2.152	−1.744	2.560	
HGB	TRS	0.41	−2.17	−1.76	2.57	

$$\mathbf{J}(\mathbf{r})_{\text{pair}}=\frac{f^2}{m_\pi^2}\sum_{i\neq j}[\tau(i)\times\tau(j)]_3\sigma(i)\delta(\mathbf{r}-\mathbf{x}_i)$$
$$\times[\sigma(j)\cdot\nabla_r]h_0(|\mathbf{r}-\mathbf{x}_j|)\,, \tag{13}$$

where

$$h_0(r)=\frac{1}{r}\left[e^{-m_\pi r}-e^{-\Lambda r}-\frac{\Lambda r}{2}\left[1-\frac{m_\pi^2}{\Lambda^2}\right]e^{-\Lambda r}\right] \tag{14}$$

and

$$f^2=0.078\,.$$

For m_π we use 0.708 fm^{-1} (140 MeV). The value of the pion-nucleon (monopole) form factor parameter Λ is more controversial, although current practice[26] suggests a value of 4.12 fm^{-1} ($5.8m_\pi$). However, we shall present results using a range of values for Λ. The sensitivity of the trinucleon magnetic moments to this parameter will then be evident.

Before proceeding, it is useful to restate several points relating to $\mathbf{J}_{\text{pair}}$. The first concerns the influence of the πN coupling model selected for the derivation of Eq. (13), i.e., pseudoscalar (PS) or pseudovector (PV). As pointed out many times in the past,[27] these couplings lead to the *same* formula for $\mathbf{J}_{\text{pair}}$ to (nonrelativistic) order f^2/m_π^2. The second involves the disparities that can arise when different electromagnetic form factors are used in the two couplings. As discussed by Lock and Foldy[28] there are reasons for associating the axial vector form factor $G_A(q^2)/G_A(0)\equiv F_A(q^2)$ with the contact term that arises in the PV theory. Then the difference between the pair current calculated in each theory would be proportional to

$$\frac{f^2}{m_\pi^2}[F_1^v(q^2)-F_A(q^2)]\,.$$

In any case, such a term would not contribute to $\mu(q=0)$. A final point concerns the cutoff parameter Λ and the gauge invariance of the theory. Strictly speaking, gauge invariance holds only for the case $\Lambda=\infty$. However, by altering the definition of the pion-nucleon form factor such that gauge invariance holds for finite Λ, Maize and Kim[9] found that the overall effect on magnetic form factors is small. They estimate an effect on the trinucleon magnetic moments of about 1%. Their prescription for restoring gauge invariance is not unique, however, and making no changes in the *solenoidal* part of the current is also acceptable.[29]

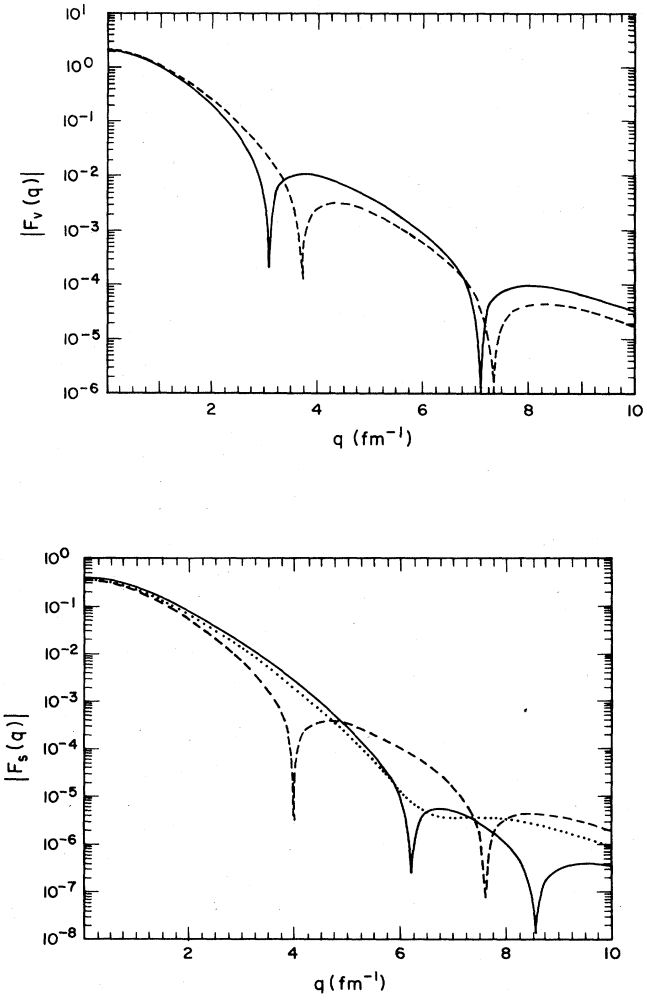

FIG. 3. (a) Impulse approximation isovector component $F_v(q)$ of the magnetic form factor $\mu(q)$. Dashed, dotted, and solid lines depict form factors computed using the densities ρ_σ, $\rho_\sigma+\rho_{L_z}$, and $\rho_\sigma+\rho_{L_z}+\rho_{Y\sigma}$. In this figure, the dashed and dotted lines are indistinguishable. (b) Impulse approximation isoscalar component $F_s(q)$ of the magnetic form factor $\mu(q)$. Labeling of curves is as described for Fig. 2(a).

The magnetic density corresponding to $\mathbf{J}_{\text{pair}}$ is denoted by ρ_{pair}. It is given in terms of the trinucleon wave function by (P waves omitted)

TABLE II. Partial wave contributions to μ_{pair}. Entries calculated using $\Lambda=5.8m_\pi$.

	RSCC	RSC	AV14	SSCC	TRS	MT13
S-S	−0.244	−0.249	−0.258	−0.262	−0.263	−0.301
S-D	−0.082	−0.084	−0.086	−0.082	−0.085	
D-D	0	0	0	0	0	

$$\rho_{\rm pair}(r)=(2T_3)6(f^2/m_\pi^2)\frac{4\pi}{3}\int d^3x\,d^3y\,\delta(\mathbf{r}+\tfrac{2}{3}\mathbf{y})h_0'(\,|\,\mathbf{r}-\tfrac{1}{2}\mathbf{x}-\tfrac{1}{3}\mathbf{y}\,|\,)$$
$$\times\{(r^2+\tfrac{1}{3}rx\mu)(u^2-v_1^2-v_2^2)+2[r^2P_2(\mu)+\tfrac{1}{3}rxP_1(\mu)](v_2v_4^I+uv_3^I-v_1v_3^I)$$
$$-2(r^2+\tfrac{1}{3}rxP_1)(v_1v_3^J-v_2v_4^J-uv_3^J)+2[\tfrac{5}{9}(1+\tfrac{1}{5}P_2)rx+2r^2\mu]$$
$$\times(v_2v_4^K+uv_3^K-v_1v_3^K)\}\,, \tag{15}$$

where

$$h_0'(z)=\frac{1}{z}\frac{d}{dz}h_0(z)\,.$$

This result is more conveniently expressed in the I,J,K representation[20] of the D waves than the L,M,K representation used earlier in Eqs. (8), (9), (10), and (11).

We illustrate the density $\rho_{\rm pair}$ in Fig. 4 for the case of $\Lambda=5.8m_\pi$. It is clear that $\rho_{\rm pair}$ does not have a strong dependence on the wave function. This is probably due to the fact that the dominant contributions to $\rho_{\rm pair}$ arise from S-S matrix elements. We elaborate on this in Table II by detailing the pair term contributions to the magnetic moment from the S-S, S-D, and D-D matrix elements. The D-D matrix elements vanish because of isospin permutation symmetry.

We postpone giving the final pair term results until after our discussion of the pion current, because some authors have given their results as a summed pair plus pion effect.

IV. THE PION CURRENT TERM

The pion current [see Fig. 1(b)] or true-exchange current is given by

$$\mathbf{J}_\pi(\mathbf{r})=\frac{-f^2}{8\pi m_\pi^2}\sum_{i\neq j}[\tau(i)\times\tau(j)]_3[\sigma(i)\cdot\nabla_r h_0(\,|\,\mathbf{r}-\mathbf{x}_i\,|\,)]\overleftrightarrow{\nabla}_r$$
$$\times[\sigma(j)\cdot\nabla_r h_0(\,|\,\mathbf{r}-\mathbf{x}_j\,|\,)]\,. \tag{16}$$

This current differs from the pair current and Δ-isobar current in one essential way—it is not localized at the point where the nucleon absorbs the photon. That is, there is no factor like $\delta(\mathbf{r}-\mathbf{x}_i)$ in the current. Such a factor permits one to reduce the calculation of $\rho_{\rm mag}(r)$ to a two-dimensional integral. Without it, however, as in the case of $\mathbf{J}_\pi$, the numerical calculation of $\rho_{\rm mag}(r)$ involves a time-consuming multidimensional integral for each value of r. For this reason, we have not calculated $\rho_\pi(r)$. However, because we only focus on the magnetic moment, μ_π, due to the pion current, our problem simplifies immensely. We obtain the following expression for μ_π:

$$\mu_\pi=\tfrac{1}{2}\int d^3r[\mathbf{r}\times\mathbf{J}_\pi(\mathbf{r})]_z$$
$$=3\frac{f^2}{m_\pi^2}\pi\int dx\,dy\,d\mu\,x^2y^2\left[-\tfrac{4}{3}(G'+\tfrac{1}{3}x^2G'')(u^2-v_1^2-v_2^2)+\tfrac{4}{9}xG''\left[\frac{2}{\sqrt{3}}\mu yT^I+xU^I\right]\right.$$
$$+\frac{4}{9}\left[\frac{2}{\sqrt{3}}\mu xyG''+\frac{1}{\sqrt{3}}\mu(1-\mu^2)x^3yG'''\right]T^J+\tfrac{4}{9}x^2G''U^JP_2$$
$$\left.+\tfrac{8}{9}x^2G''\mu U^K+\frac{4}{45\sqrt{3}}(5xyG''+x^3yG''')(3+\mu^2)T^K-\frac{16}{45\sqrt{3}}x^3yG'''P_2(\mu)T^K\right]\,, \tag{17}$$

where

$$G(x)=\frac{e^{-\Lambda x}}{\Lambda}+\frac{e^{-m_\pi x}}{m_\pi}-\frac{4}{(\Lambda^2-m_\pi^2)x}(e^{-m_\pi x}-e^{-\Lambda x})\,,$$
$$G'=\frac{1}{x}\frac{dG}{dx}\,,$$
$$G''=\frac{1}{x}\frac{dG'}{dx}\,,$$

and

$$G'''=\frac{1}{x}\frac{dG''}{dx}\,.$$

The quantities T^I, U^I, etc., are defined below by Eqs. (29) and (30). Multiplication by $2M_pc/\hbar=9.51$ converts the dimensions of μ_π from fm to nuclear magnetons.

Table III enumerates the partial wave contributions to μ_π. We note that, as in the pair current, the S-S matrix elements are dominant and the D-D matrix elements vanish identically. (Both the pair and pion currents contain the same isospin factor $[\tau(i)\times\tau(j)]_3$.)

Our results for $\mu_{\rm pair}$ and μ_π calculated using $\Lambda=5.8m_\pi$ are collected in Table IV. Comparison with previous work is complicated by the Λ dependence of these quantities and by the fact that not all authors have used the same value for Λ. Fortunately, the Λ dependence is not severe for these terms, as we illustrate in Table V for the RSC model. Finally, we present in Table VI a comparison of our results with those of others.

TABLE III. Partial wave contributions to μ_π. Entries calculated using $\Lambda=5.8m_\pi$ and $(2T_3)=1$.

	RSCC	RSC	AV14	SSCC	TRS	MT13
S-S	0.106	0.109	0.115	0.118	0.120	0.140
S-D	−0.024	−0.024	−0.023	−0.022	−0.023	
D-D	0	0	0	0	0	

It is evident from Table VI that substantial agreement exists for the contributions to μ from the pair and pion currents. As mentioned previously, these contributions are due mainly to the *S*-state component of the wave function. Thus, one does not expect to see much variation in the results. It should be pointed out, however, that some calculations of μ_π, e.g., that of TG, use an approximation described as "keeping only the translationally invariant parts of the operator." This approximation, to our knowledge, first appeared in the pioneering work of Chemtob and Rho.[24] In order to describe this approximation, we first display the operator μ_π:

$$\begin{aligned}\mu_\pi=-3(32\pi^4)\frac{f^2}{m_\pi^2}[\tau(2)\times\tau(3)]_3 4\pi i\Big\{&\sqrt{2}[[\sigma(2)\otimes\sigma(3)]^1\otimes[Y_0(\hat{x})\otimes Y_0(\hat{y})]^0]_0^1(G'+\tfrac{1}{3}x^2G'')\\&+\frac{x^2}{3}[[\sigma(2)\otimes\sigma(3)]^1\otimes[Y_2(\hat{x})\otimes Y_0(\hat{y})]^2]_0^1G''(x)\\&+\tfrac{5}{9}\sqrt{2/3}xy[[\sigma(2)\otimes\sigma(3)]^0\otimes[Y_1(\hat{x})\otimes Y_1(\hat{y})]^1]_0^1G''(x)\\&-\tfrac{1}{9}\sqrt{10/3}xy[[\sigma(2)\otimes\sigma(3)]^2\otimes[Y_1(\hat{x})\otimes Y_1(\hat{y})]^1]_0^1G''(x)\\&+\tfrac{1}{9}\sqrt{10}xy[[\sigma(2)\otimes\sigma(3)]^2\otimes[Y_1(\hat{x})\otimes Y_1(\hat{y})]^2]_0^1G''(x)\\&+\tfrac{1}{9}\sqrt{2/3}x^3y[[\sigma(2)\otimes\sigma(3)]^0\otimes[Y_1(\hat{x})\otimes Y_1(\hat{y})]^1]_0^1G'''(x)\\&-\tfrac{1}{9}\sqrt{2/15}x^3y[[\sigma(2)\otimes\sigma(3)]^2\otimes[Y_1(\hat{x})\otimes Y_1(\hat{y})]^1]_0^1G'''(x)\\&+\tfrac{1}{9}\sqrt{2/5}x^3y[[\sigma(2)\otimes\sigma(3)]^2\otimes[Y_1(\hat{x})\otimes Y_1(\hat{y})]^2]_0^1G'''(x)\\&+\tfrac{1}{9}\sqrt{4/15}x^3y[[\sigma(2)\otimes\sigma(3)]^2\otimes[Y_3(\hat{x})\otimes Y_1(\hat{y})]^2]_0^1G'''(x)\\&-\tfrac{2}{9}\sqrt{2/15}x^3y[[\sigma(2)\otimes\sigma(3)]^2\otimes[Y_3(\hat{x})\otimes Y_1(\hat{y})]^3]_0^1G'''(x)\Big\}.\end{aligned}\tag{18}$$

We note that the operator is *manifestly* translationally invariant because it only depends on the relative coordinates **x** and **y**. The first two terms within the curly braces do not depend on **y**, whereas all subsequent terms depend linearly on **y**. The approximation referred to above consists of dropping all terms depending linearly on **y**. The improper nomenclature, "translationally noninvariant terms," refers to these dropped terms, presumably because in a system where the nuclear c.m. is located at the origin, i.e., $\mathbf{R}=0$, then $\mathbf{y}=\frac{3}{2}(\mathbf{r}_2+\mathbf{r}_3)=3\mathbf{R}_{23}$ is proportional to the center of mass of the 2-3

TABLE IV. Pair, pion, and isobar current contributions to μ in nuclear magnetons. These entries are for $(2T_3)=1$ and $\Lambda=5.8\mu_\pi$.

	RSCC	RSC	AV14	SSCC	TRS	MT13
μ_{pair}	−0.330	−0.338	−0.349	−0.348	−0.353	−0.301
μ_π	0.083	0.086	0.093	0.097	0.098	0.140
μ_Δ	−0.092	−0.095	−0.095	−0.085	−0.091	

pair. It does appear, however, that keeping only the first two terms of Eq. (18), i.e., the $[Y_0(\hat{x})\otimes Y_0(\hat{y})]$ and the $[Y_2(\hat{x})\otimes Y_0(\hat{y})]$ pieces, is a very good approximation. This is primarily because the first term is the only piece which has a nonzero S-S matrix element. Recall that Table III shows that S-S matrix elements provide the dominant contributions to μ_π. For example, if we compute μ_π using only the first two terms of Eq. (18), we obtain $\mu_\pi=0.074(\Lambda=8.6m_\pi$, RSC), whereas retaining all terms of the operator yields the result in Table V, $\mu_\pi=0.082$. The difference arises because the second term, $[Y_2(\hat{x})\otimes Y_0(\hat{y})]$, does not pick up the complete S-D contribution.

V. THE Δ-ISOBAR CURRENT

The current due to virtual photoexcitation of the 3-3 resonance on one nucleon with its subsequent decay by pion emission [see Fig. 1(c)] is denoted $\mathbf{J}_\Delta(\mathbf{r})$. It is given in the static Δ-propagator approximation by

$$\mathbf{J}_\Delta(\mathbf{r})=-\frac{8}{25}\frac{f^2}{m_\pi^2}\frac{\mu_p-\mu_n}{2M_p(M_\Delta-M_p)}\nabla\times\sum_{i\neq j}\delta(\mathbf{r}-\mathbf{x}_i)\cdot\{[\boldsymbol{\sigma}(i)\times\nabla_r][\boldsymbol{\tau}(i)\times\boldsymbol{\tau}(j)]_3-4\tau_3(j)\nabla_r\}\boldsymbol{\sigma}(j)\cdot\nabla_r h_0(|\mathbf{r}-\mathbf{x}_j|)\,. \tag{19}$$

It should be noted that this current is solenoidal and hence is automatically conserved, independent of the form of h_0. However, there does appear to be some latitude in the choice of the $\gamma N\Delta$ coupling constant used to derive $\mathbf{J}_\Delta$. That used in Eq. (19) is the value obtained by Riska and Brown using the static quark model. Thakur and Foldy,[30] on the other hand, obtain $\frac{5}{4}$ times this result on the basis of a correct treatment of pion rescattering in the Chew-Low model. Chemtob and Rho[24] used a dispersion theory analysis of πN scattering in the Δ and Roper channels and obtained slightly different coupling constants. Using their values, the overall current of Eq. (19) would increase by 6% and the factor of 4 multiplying the $\tau_3(j)\nabla_r$ term in the curly braces would be replaced by 3.56. We shall see that this uncertainty in the coupling constant is insignificant compared to the dependence of μ_Δ on Λ.

Unfortunately the expression for ρ_Δ is algebraically complicated and, as a result, not that illuminating. We include it (without the P waves) for completeness.

$$\rho_\Delta(r)=(2T_3)r\left[\frac{d}{dr}F_0(r)+\sqrt{5/2}\left[\frac{d}{dr}+\frac{3}{r}\right]F_2(r)\right], \tag{20}$$

$$\begin{aligned}F_0(r)=&\frac{16\pi}{25}\frac{f^2}{m_\pi^2}\frac{(\mu_p-\mu_n)}{2M_p(M_\Delta-M_p)}3\int d^3x\,d^3y\,\delta(\mathbf{r}+\tfrac{2}{3}\mathbf{y})\\
&\times\left\{\left[\frac{4}{\sqrt{3}}v_1v_2-\tfrac{4}{3}v_2^2\right][\tfrac{16}{9}h_0'+\tfrac{4}{3}(r^2+\tfrac{1}{9}x^2+\tfrac{2}{3}xrP_1)h_0'']+\tfrac{8}{3}(r^2P_2+\tfrac{1}{9}x^2+\tfrac{2}{3}xrP_1)W^Ih_0''\right.\\
&+\tfrac{8}{3}(r^2+\tfrac{1}{9}x^2P_2+\tfrac{2}{3}xrP_1)W^Jh_0''+\tfrac{16}{3}[(r^2+\tfrac{1}{9}x^2)P_1+\tfrac{1}{9}xr(5+P_2)]W^Kh_0''\\
&-\tfrac{32}{27}[Y^{I,I}+Y^{J,J}+(3+\mu^2)Y^{K,K}]h_0'-\tfrac{8}{9}[r^2(1-2P_2)-\tfrac{1}{9}x^2-\tfrac{2}{3}xrP_1]Y^{I,I}h_0''\\
&+\tfrac{16}{9}[(r^2+\tfrac{1}{9}x^2)P_2+\tfrac{2}{3}xrP_1]Y^{I,J}h_0''+\tfrac{32}{45}[r^2(2P_1+3P_3)+\tfrac{5}{9}x^2P_1+\tfrac{5}{9}xr(5+P_2)]Y^{I,K}h_0''\\
&+\tfrac{8}{9}[r^2-\tfrac{1}{9}x^2(1-2P_2)+\tfrac{2}{3}xrP_1]Y^{J,J}h_0''+\tfrac{32}{9}[r^2P_1+\tfrac{1}{45}x^2(2P_1+3P_3)+\tfrac{1}{9}xr(5+P_2)]Y^{J,K}h_0''\\
&\left.+\tfrac{32}{27}[(r^2+\tfrac{1}{9}x^2)(1+2P_2)+\tfrac{2}{5}xr(6P_1-P_3)]Y^{K,K}h_0''+\tfrac{32}{27}(1-3\mu^2)Y^{I,J}h_0'-\tfrac{128}{27}\mu(Y^{I,K}+Y^{J,K})h_0'\right\},\end{aligned} \tag{21}$$

where

$$W^\alpha=\tfrac{8}{3}v_4^\alpha v_2+\sqrt{3}v_4^\alpha u-\frac{1}{\sqrt{3}}(v_4^\alpha v_1+v_3^\alpha v_2)\,,\quad \alpha=I,J,K\,, \tag{22}$$

$$Y^{\alpha,\beta}=v_4^\alpha v_4^\beta-\frac{\sqrt{3}}{2}(v_4^\alpha v_3^\beta+v_4^\beta v_3^\alpha)\,, \tag{23}$$

$$h_0''=\frac{1}{z}\frac{d}{dz}h_0'=\frac{1}{z}\frac{d}{dz}\left[\frac{1}{z}\frac{d}{dz}h_0\right], \tag{24}$$

and $P_l(\mu)$ are Legendre polynomials.

Similarly, the S-S, S-D, and D-D contributions to $F_2(r)$ are given by:

$$F_2(r)=\frac{16\pi}{25}\frac{f^2}{m_\pi^2}\frac{(\mu_p-\mu_n)}{2M_p(M_\Delta-M_p)}3\int d^3x\,d^3y\,\delta(\mathbf{r}+\tfrac{2}{3}\mathbf{y})$$
$$\times\Bigg[\frac{4}{3\sqrt{10}}(r^2+\tfrac{1}{9}x^2P_2+\tfrac{2}{3}xrP_1)\left[3u^2-3v_1^2-\tfrac{1}{3}v_2^2-\frac{8}{\sqrt{3}}v_1v_2\right]h_0''+\frac{8}{3\sqrt{30}}[(3\mu^2-1)Z^I+2Z^J+4\mu Z^K]h_0'+\frac{2}{\sqrt{30}}$$
$$\times\{[(r^2+\tfrac{1}{9}x^2)P_2+\tfrac{2}{3}rxP_1+\tfrac{3}{5}rxP_3]S_1^I-[(r^2+\tfrac{1}{9}x^2)P_2+\tfrac{7}{15}rxP_1+\tfrac{1}{5}rxP_3]S_2^I\}h_0''$$
$$+\frac{2}{\sqrt{30}}\{[r^2+\tfrac{1}{9}x^2(2-P_2)+\tfrac{2}{3}rxP_1]S_1^J-(r^2+\tfrac{1}{9}x^2P_2+\tfrac{2}{3}rxP_1)S_2^J\}h_0''$$
$$+\frac{4}{\sqrt{30}}\{[\tfrac{1}{18}xr(1+11P_2)+r^2P_1+\tfrac{1}{90}x^2(13P_1-3P_3)]S_1^K$$
$$-[\tfrac{1}{18}xr(7+5P_2)+r^2P_1+\tfrac{1}{90}x^2(7P_1+3P_3)]S_2^K\}h_0''$$
$$-\tfrac{8}{3}\sqrt{2/5}[(r^2+\tfrac{1}{9}x^2)P_2+\tfrac{1}{30}xr(11P_1+9P_3)]X^Ih_0''-\tfrac{8}{3}\sqrt{2/5}[r^2+\tfrac{1}{18}x^2(1+P_2)+\tfrac{2}{3}xrP_1]X^Jh_0''$$
$$-\tfrac{4}{3}\sqrt{2/5}[\tfrac{1}{9}xr(11+13P_2)+4r^2P_1+\tfrac{1}{45}x^2(17P_1+3P_3)]X^Kh_0''$$
$$+\frac{32}{27\sqrt{10}}[(1-3\mu^2)Y^{I,I}+2(1-3\mu^2)Y^{I,J}-6\mu(\mu^2+\tfrac{1}{3})Y^{I,K}-2Y^{J,J}-8\mu Y^{J,K}-(3+5\mu^2)Y^{K,K}]h_0'$$
$$+\frac{16}{9\sqrt{10}}[r^2(1-2P_2)-\tfrac{1}{9}x^2P_2-\tfrac{1}{15}xr(P_1+9P_3)]Y^{I,I}h_0''$$
$$-\frac{16}{9\sqrt{10}}[2r^2P_2+\tfrac{1}{9}x^2(1+P_2)+\tfrac{1}{15}xr(11P_1+9P_3)]Y^{I,J}h_0''$$
$$-\frac{128}{45\sqrt{10}}[r^2(P_1+\tfrac{3}{2}P_3)+\tfrac{1}{72}x^2(17P_1+3P_3)+\tfrac{1}{504}xr(259+365P_2+216P_4)]Y^{I,K}h_0''$$
$$-\frac{16}{9\sqrt{10}}(r^2+\tfrac{1}{9}x^2+\tfrac{2}{3}xrP_1)Y^{J,J}h_0''$$
$$-\frac{16}{9\sqrt{10}}[4r^2P_1+\tfrac{1}{45}x^2(23P_1-3P_3)+\tfrac{1}{9}xr(11+13P_2)]Y^{J,K}h_0''$$
$$-\frac{8}{27\sqrt{10}}[8r^2(1+2P_2)+\tfrac{1}{315}x^2(364+620P_2-144P_4)+4xr(3P_1+P_3)]Y^{K,K}h_0''\Bigg], \tag{25}$$

where

$$Z^\alpha=-v_4^\alpha u-\frac{7}{3\sqrt{3}}v_4^\alpha v_2+\sqrt{3}(v_3^\alpha u-v_3^\alpha v_1)$$
$$+\tfrac{5}{3}(v_3^\alpha v_2+v_4^\alpha v_1), \tag{26}$$
$$X^\alpha=\sqrt{3}v_4^\alpha u+\tfrac{5}{3}v_4^\alpha v_2-(v_3^\alpha u-v_3^\alpha v_1)$$
$$-\frac{1}{\sqrt{3}}(v_3^\alpha v_2+v_4^\alpha v_1), \tag{27}$$
$$S_1^\alpha=T^\alpha+\frac{1}{\sqrt{3}}U^\alpha,\quad S_2^\alpha=T^\alpha-\sqrt{3}U_\alpha, \tag{28}$$
$$T^\alpha=v_4^\alpha u+v_4^\alpha v_1+v_3^\alpha v_2, \tag{29}$$
$$U^\alpha=v_4^\alpha v_2+v_3^\alpha u-v_3^\alpha v_1. \tag{30}$$

The derivatives of F_0 and F_2 were computed by fitting a cubic spline to each of these functions. Note that F_2 does not contribute to μ_Δ.

TABLE V. Λ variation of μ_{pair} and μ_π for the RSC potential.

$\Lambda(m_\pi)$	μ_{pair}	μ_π	$\mu_{\text{pair}}+\mu_\pi$
2.0	−0.241	+0.036	−0.205
4.0	−0.333	+0.081	−0.252
5.8	−0.338	+0.086	−0.252
8.6	−0.334	+0.082	−0.252
17.2	−0.330	+0.072	−0.258

TABLE VI. Comparison of μ_π and μ_{pair} computed by others to the present work. All calculations use the RSC potential.

Reference	μ_{pair}	μ_π	$\mu_{\text{pair}}+\mu_\pi$
HKTR ($\Lambda=\infty$)			−0.241
present ($\Lambda=17.2m_\pi$)			−0.258
SHS ($\Lambda=8.6m_\pi$)	−0.33	0.07	−0.26
present ($\Lambda=8.6m_\pi$)	−0.334	0.082	−0.252
MK ($\Lambda=4m_\pi$)	−0.33	0.11	−0.22
present ($\Lambda=4m_\pi$)	−0.333	0.081	−0.251
TG ($\Lambda=\infty$)			−0.246
present ($\Lambda=17.2m_\pi$)			−0.258

TABLE VII. Partial wave contributions to μ_Δ. Entries calculated using $\Lambda=5.8m_\pi$.

	RSCC	RSC	AV14	SSCC	TRS	MT13
S-S	0.000	0.000	0.000	0.000	0.000	0.000
S-D	−0.091	−0.093	−0.093	−0.083	−0.089	
D-D	−0.002	−0.003	−0.003	−0.002	−0.003	

TABLE VIII. Comparison of μ_Δ computed by others to the present (RSC) calculation. SHS find −0.145 in a static approximation which corresponds to our treatment.

Reference	μ_Δ
HKTR ($\Lambda=\infty$)	−0.166
present ($\Lambda=17.2m_\pi$)	−0.172
SHS ($\Lambda=8.6m_\pi$)	−0.05
present ($\Lambda=8.6m_\pi$)	−0.135
MK ($\Lambda=4m_\pi$)	−0.036
present ($\Lambda=4m_\pi$)	−0.057
TG ($\Lambda=\infty$)	−0.175
present ($\Lambda=17.2m_\pi$)	−0.172

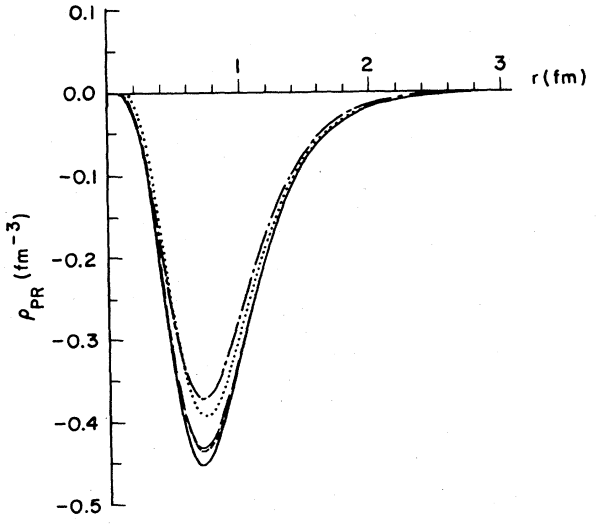

FIG. 4. ρ_{pair} computed using various NN potentials. Dash-dot, dotted, long dash, short dash, and solid curves are for the potentials MT13, RSCC, SSCC, AV14, and TRS, respectively.

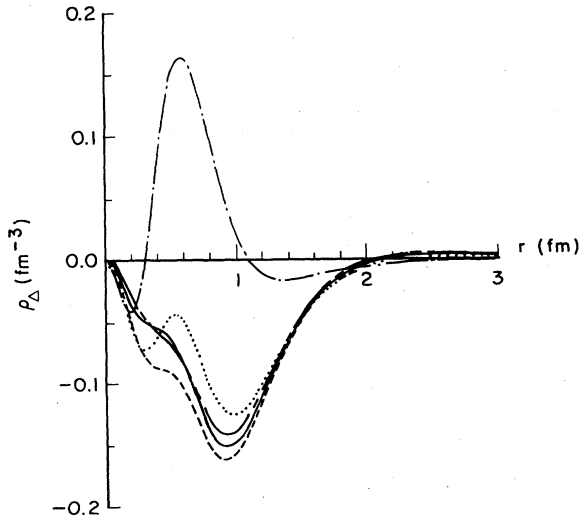

FIG. 5. ρ_Δ computed using various NN potentials. Labeling of the curves is as described in Fig. 4.

TABLE IX. Summary of our magnetic moment calculations. Entries are calculated using $\Lambda=5.8m_\pi$.

Potential	BE (MeV)	μ_s	μ_v	$\mu(^3\text{He})$	$\mu(^3\text{H})$
RSCC	6.41	0.405	−2.482	−2.077	2.886
RSC	7.02	0.405	−2.496	−2.091	2.900
AV14	7.44	0.405	−2.516	−2.111	2.921
SSCC	7.46	0.409	−2.515	−2.105	2.924
TRS	7.49	0.407	−2.512	−2.105	2.919
MT13	8.53	0.440	−2.453	−2.013	2.893
Experiment		0.4257	−2.5532	−2.1275	2.9789

Table VII displays the partial wave contributions to μ_Δ. It is evident from this table that the S-D overlap is almost the sole contributor to μ_Δ. The S-S contribution is listed as 0.000 to indicate that it is very small, but certainly not identically zero. In fact, one can see from Fig. 5, where ρ_Δ is plotted as a function of r, that S-S matrix elements have a sizable effect on the magnetic density. To see this, one should note that the potential model MT has only S states. Certainly much more model dependence is evident in ρ_Δ than in ρ_{pair}. The variation with Λ is also more severe in the case of μ_Δ. We illustrate this in Fig. 6, where a cubic spline is fitted to five values of μ_Δ calculated with different Λ's. It is apparent from this curve that the $\Lambda\to\infty$ value of μ_Δ must be almost the same as our $\Lambda=17.2m_\pi$ value.

Our results for the total contribution to μ_Δ are contained in Table IV. Comparing these results with those in Table VII shows that the P-wave contributions do not contribute significantly. The comparison with other authors is given in Table VIII. One notes from this table a disparity with our results and those of SHS. However, as pointed out in the Introduction, SHS's calculation contains a more refined isobar contribution (a nonstatic Δ propagator). The comparison is nonetheless instructive, since it gives an idea of the importance of a more realistic treatment of the Δ propagator. The small disagreement with MK probably is a result of their use of a parametrized wave function.

VI. CONCLUSIONS

Table IX summarizes our results for the six potential models we have chosen. The ^{3}H binding energy varies from 6.41 to 7.49 MeV for those potentials which include a tensor force. We see that this $\approx 15\%$ variation in the binding energy is accompanied by a less than 2% variation in the magnetic moments. Thus, the influence of binding on the magnetic moments appears relatively unimportant.

Table X compares our calculations with the results of others. In addition, this table shows the Λ dependence of the magnetic moments since it gives our RSC results for $\Lambda=4m_\pi$, $8.6m_\pi$, and $17.2m_\pi$. This variation in Λ produces about a 5% variation in the magnetic moments. Table V shows that $\mu_{\text{pair}}+\mu_\pi$ is essentially independent of Λ; it is the isobar current which is responsible for the sensitivity of the magnetic moments to Λ.

In comparing with others, it is possible in most cases to pinpoint the areas of disagreement where any exist. We are in essential agreement with HKTR. The only difference between our results and those of SHS is in the contribution from the Δ isobar. As pointed out previously, their nonstatic treatment of the Δ propagator gives a value for μ_Δ of only one-third of our value. This results in an approximate difference of about 3% in our magnetic moments. Our small disagreement with MK seems to arise from their use of approximate RSC wave functions.

TABLE X. Comparison of magnetic moments computed by others to our own calculations.

Reference	Potential	μ_s	μ_v	$\mu(^3\text{He})$	$\mu(^3\text{H})$
HKTR ($\Lambda=\infty$)	RSC	0.408	−2.559	−2.151	2.967
present ($\Lambda=17.2m_\pi$)		(0.405)	(−2.579)	(−2.174)	(2.983)
SHS ($\Lambda=8.6m_\pi$)	RSC	0.40	−2.47	−2.07	2.87
present ($\Lambda=8.6m_\pi$)		(0.405)	(−2.536)	(−2.131)	(2.941)
MK ($\Lambda=4m_\pi$)	RSC	0.365	−2.451	−2.086	2.816
present ($\Lambda=4m_\pi$)		(0.405)	(−2.458)	(−2.053)	(2.863)
HGB ($\Lambda=8.5m_\pi$)	TRS	0.414	−2.602	−2.188	3.016
present ($\Lambda=8.6m_\pi$)		(0.407)	(−2.548)	(−2.141)	(2.955)
TG ($\Lambda=\infty$)	RSC	0.397	−2.529	−2.132	2.927
present ($\Lambda=17.2m_\pi$)		(0.405)	(−2.579)	(−2.174)	(2.983)

This approximation leads to a larger error to their impulse approximation results than in their exchange current results. We are cognizant of the fact that MK were addressing themselves more to questions regarding current conservation and that, for their purposes, the approximate wave functions were sufficient. It has nevertheless been beneficial for us to have their work to compare with, especially the individual exchange current pieces which agree quite closely with our own.

It appears from our work that the greatest source of uncertainty in calculating trinucleon magnetic moments is in the treatment of the Δ isobar. This term is sensitive to both the parameter Λ and to the treatment of the Δ propagator. In addition, there are various prescriptions for choosing the γN coupling constant used in Eq. (19). Our rough estimate of the uncertainty in this process is $\pm 50\%$ or $-0.09 \pm 0.05\ \mu_N$. The additional small short-range contributions[10,22] tend to increase μ_v and thus improve agreement between theory and experiment, if one uses the preferred[26] value of $\Lambda/m_\pi = 5.8$.

We note again that our calculations have included only pion-range exchange current operators. We have ignored all other meson exchange currents, which are of shorter range. One consequence of this choice is that all of our exchange currents are isovector, and the isoscalar currents are determined by the impulse approximation. Moreover, the underlying dynamics and all the electromagnetic current operators are nonrelativistic in nature. We expect modifications to the magnetic moments of the order of a few percent from relativistic corrections.

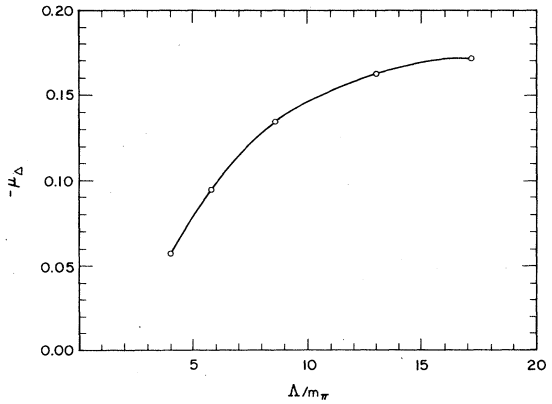

FIG. 6. Variation of μ_Δ with Λ. These points were computed using the RSC model.

ACKNOWLEDGMENTS

The work of E. L. Tomusiak and M. Kimura was supported by the Natural Sciences and Engineering Research Council of Canada. The work of J. L. Friar and B. F. Gibson was performed under the auspices of the U.S. Department of Energy, while G. L. Payne and J. Dubach were supported in part by the U.S. Department of Energy.

[1]S. D. Drell and J. D. Walecka, Phys. Rev. **120**, 1069 (1960).
[2]J. L. Friar, Phys. Rev. C **27**, 2078 (1983).
[3]D. O. Riska and G. E. Brown, Phys. Lett. **38B**, 193 (1972).
[4]G. G. Simon, F. Borkowski, Ch. Schmitt, V. H. Walther, H. Arenhövel, and W. Fabian, Phys. Rev. Lett. **37**, 739 (1976); also see M. Bernheim *et al.*, *ibid.* **46**, 402 (1981); J. Hockert, D. O. Riska, M. Gari, and A. Huffman, Nucl. Phys. **A217**, 14 (1973).
[5]R. G. Sachs and J. Schwinger, Phys. Rev. **70**, 41 (1946).
[6]E. Gerjuoy and J. Schwinger, Phys. Rev. **61**, 138 (1942).
[7]E. P. Harper, Y. E. Kim, A. Tubis, and M. Rho, Phys. Lett. **40B**, 533 (1972).
[8]D. O. Riska, Nucl. Phys. **A350**, 227 (1980).
[9]M. A. Maize and Y. E. Kim, Nucl. Phys. **A420**, 365 (1984).
[10]W. Strueve, Ch. Hajduk, and P. U. Sauer, Nucl. Phys. **A405**, 620 (1983). Note: their value of μ_π quoted herein obtained by private communication with P. Sauer.
[11]J. Torre and B. Goulard, Phys. Rev. C **28**, 529 (1983).
[12]R. V. Reid, Jr., Ann. Phys. (N.Y.) **50**, 411 (1968); B. Day, Phys. Rev. C **24**, 1203 (1981).
[13]R. B. Wiringa, R. A. Smith, and T. A. Ainsworth, Phys. Rev. C **29**, 1207 (1984).
[14]R. de Tourreil and D. W. L. Sprung, Nucl. Phys. **A201**, 193 (1984).
[15]R. de Tourreil, B. Rouben, and D. W. L. Sprung, Nucl. Phys. **A242**, 445 (1975).
[16]R. A. Malfliet and J. A. Tjon, Nucl. Phys. **A127**, 161 (1969).
[17]G. L. Payne, J. L. Friar, and B. F. Gibson, Phys. Rev. C **22**, 832 (1980) contains the RSC Coulomb case.
[18]C. R. Chen, G. L. Payne, J. L. Friar, and B. F. Gibson, Phys. Rev. C **31**, 2266 (1985).
[19]G. L. Payne, J. L. Friar, and B. F. Gibson, and I. R. Afnan, Phys. Rev. C **22**, 823 (1980) contains the MTI–III case. Note that this potential differs somewhat from the original.
[20]J. L. Friar, E. L. Tomusiak, B. F. Gibson, and G. L. Payne, Phys. Rev. C **24**, 677 (1981).
[21]J. Torre, B. Goulard, and E. Hadjimichael (private communication).
[22]E. Hadjimichael, B. Goulard, and R. Bornais, Phys. Rev. C **27**, 831 (1983).
[23]R. A. Brandenburg, Y. E. Kim, and A. Tubis, Phys. Rev. Lett. **32**, 1325 (1974).
[24]M. Chemtob and M. Rho, Nucl. Phys. **A163**, 1 (1971).
[25]J. L. Friar, Ann. Phys. (N.Y.) **104**, 380 (1977).
[26]S. A. Coon and M. D. Scadron, Phys. Rev. C **23**, 1150 (1981).
[27]See the discussion and references quoted in Ref. 25.
[28]J. A. Lock and L. L. Foldy, Ann. Phys. (N.Y.) **93**, 276 (1975).
[29]J. L. Friar and S. Fallieros, Phys. Lett. **114B**, 403 (1982); Phys. Rev. C **29**, 1645 (1984).
[30]J. Thakur and L. L. Foldy, Phys. Rev. C **8**, 1957 (1973).